

DNAJB9 Is a Specific Immunohistochemical Marker for Fibrillary Glomerulonephritis



Samih H. Nasr^{1,6}, Julie A. Vrana^{1,6}, Surendra Dasari², Frank Bridoux³, Mary E. Fidler¹, Sihem Kaaki⁴, Nathalie Quellard⁴, Alexia Rinsant⁴, Jean Michel Goujon⁴, Sanjeev Sethi¹, Fernando C. Fervenza⁵, Lynn D. Cornell¹, Samar M. Said¹, Ellen D. McPhail¹, Loren P. Herrera Hernandez¹, Joseph P. Grande¹, Marie C. Hogan⁵, John C. Lieske^{1,5}, Nelson Leung⁵, Paul J. Kurtin^{1,7} and Mariam P. Alexander^{1,7}

¹Department of Laboratory Medicine and Pathology, Mayo Clinic, Rochester, Minnesota, USA; ²Department of Health Sciences Research, Mayo Clinic, Rochester, Minnesota, USA; ³Department of Nephrology, Dialysis and Renal Transplantation, University Hospital of Poitiers, Centre de référence de l'amylose AL et des autres maladies par dépôts d'immunoglobuline monoclonale, Poitiers, France; ⁴Department of Pathology, University Hospital of Poitiers, Poitiers, France; and ⁵Department of Internal Medicine, Mayo Clinic, Rochester, Minnesota, USA

Introduction: Fibrillary glomerulonephritis (FGN) is a rare disease with unknown pathogenesis and a poor prognosis. Until now, the diagnosis of this disease has required demonstration of glomerular deposition of randomly oriented fibrils by electron microscopy that are Congo red negative and stain with antisera to Igs. We recently discovered a novel proteomic tissue biomarker for FGN, namely, DNAJB9.

Methods: In this work, we developed DNAJB9 immunohistochemistry and tested its sensitivity and specificity for the diagnosis of FGN. This testing was performed on renal biopsy samples from patients with FGN (n = 84), amyloidosis (n = 21), a wide variety of non-FGN glomerular diseases (n = 98), and healthy subjects (n = 11). We also performed immunoelectron microscopy to determine whether DNAJB9 is localized to FGN fibrils.

Results: Strong, homogeneous, smudgy DNAJB9 staining of glomerular deposits was seen in all but 2 cases of FGN. The 2 cases that did not stain for DNAJB9 were unique, as they had glomerular staining for IgG only (without κ or λ) on immunofluorescence. DNAJB9 staining was not observed in cases of amyloidosis, in healthy subjects, or in non-FGN glomerular diseases (with the exception of very focal staining in 1 case of smoking-related glomerulopathy), indicating 98% sensitivity and > 99% specificity. Immunoelectron microscopy showed localization of DNAJB9 to FGN fibrils but not to amyloid fibrils or immunotactoid glomerulopathy microtubules.

Conclusion: DNAJB9 immunohistochemistry is sensitive and specific for FGN. Incorporation of this novel immunohistochemical biomarker into clinical practice will now allow more rapid and accurate diagnosis of this disease.

Kidney Int Rep (2018) 3, 56–64; <http://dx.doi.org/10.1016/j.ekir.2017.07.017>

KEYWORDS: biomarker; DNAJB9; fibrillary glomerulonephritis; immunoelectron microscopy; immunohistochemistry; kidney biopsy

© 2017 International Society of Nephrology. Published by Elsevier Inc. This is an open access article under the CC BY-NC-ND license (<http://creativecommons.org/licenses/by-nc-nd/4.0/>).

Fibrillary glomerulonephritis (FGN) is a rare disease that was first described in the literature by Rosemann and Eliakim in 1977¹ and was later recognized as a distinct glomerular disease by Duffy *et al.* in 1983.²

Current diagnostic criteria for FGN require the demonstration of haphazardly arranged, straight fibrils measuring 10 to 30 nm in thickness in the mesangium and/or along the glomerular basement membranes by electron microscopy (EM).^{3–6} On immunofluorescence (IF), in most cases, the deposits stain for IgG, both κ and λ light chains, and C3. The majority of cases show IgG4 subtype restriction. On light microscopy (LM), most cases exhibit mesangial expansion/hypercellularity, with or without duplication of the glomerular basement membranes. In the vast majority of cases of FGN, these deposits are Congo red negative, which is important in distinguishing FGN from renal amyloidosis.

Correspondence: Mariam P. Alexander, Department of Laboratory Medicine and Pathology, Mayo Clinic, 200 First Street SW, Rochester, Minnesota 55905, USA. E-mail: Alexander.Mariam@mayo.edu

⁶These authors contributed equally to this work.

⁷Co-senior authors.

Received 26 July 2017; accepted 31 July 2017; published online 7 August 2017

There are several limitations of the current means of diagnosing FGN. First, no single feature on LM, IF, or EM is pathognomonic of this disease. The LM finding of mesangial expansion and hypercellularity can be lacking in the early stage of disease and can also be seen in several other glomerular diseases such as IgA nephropathy, immunotactoid glomerulopathy, diabetic glomerulosclerosis, fibronectin glomerulopathy, and collagenofibrotic glomerulopathy. The IF findings can overlap with other forms of immune-mediated glomerulonephritis (such as lupus nephritis and membranous glomerulonephritis), with immunotactoid glomerulopathy, and with renal amyloidoses (including heavy and light chain amyloidosis, heavy chain amyloidosis, and AA amyloidosis with entrapped Igs). On EM, FGN can be difficult to distinguish from other glomerular diseases that exhibit fibrils or small microtubules, including amyloidosis, immunotactoid glomerulopathy associated with chronic lymphocytic leukemia, diabetic fibrillosis, and fibronectin glomerulopathy. Second, kidney biopsy samples may be limited, without glomeruli available for IF or EM. In these situations, a pathologic diagnosis of FGN is not possible without repeat biopsy. Third, because EM is labor intensive and expensive, it is not routinely performed in many pathology laboratories, particularly in the developing countries, and hence FGN is likely an underdiagnosed disease.

Through the use of laser microdissection–assisted liquid chromatography–tandem mass spectrometry (LMD/MS-MS), we recently discovered a novel proteomic biomarker for FGN: DnaJ homolog subfamily B member 9 (DNAJB9), a member of the molecular chaperone gene family.⁷ In this work, we developed DNAJB9 immunohistochemistry (IHC) and tested its sensitivity and specificity for the diagnosis of FGN in a large cohort of patients. We also performed immunoelectron microscopy (immuno-EM) to determine whether DNAJB9 is localized to FGN fibrils.

MATERIALS AND METHODS

Study Patients

All FGN cases included in this study fulfilled the following previously established diagnostic criteria⁵: glomerular deposition of fibrils that were (i) randomly oriented, (ii) lacked hollow centers at magnification of <30,000; (iii) were Congo-red negative; and (iv) stained with antisera to Igs by IF. **Table 1** shows the salient clinical characteristics at diagnosis and pathologic findings of the 84 Mayo Clinic FGN cases. The pathologic diagnoses of non-FGN glomerular diseases (NFGNGDs) and amyloidosis were made using current standard pathologic diagnostic criteria. Three of the

FGN cases were included in our previously published clinicopathologic series on FGN.⁵

Renal Biopsy Sample Evaluation

Standard processing of renal biopsy samples included LM, IF, and transmission EM. For LM, all renal biopsy samples were stained with hematoxylin and eosin, periodic acid–Schiff, Masson's trichrome, and Jones methenamine silver. All cases of FGN and amyloidosis were stained with Congo red. For IF, 4- μ m cryostat sections were stained with polyclonal fluorescein isothiocyanate–conjugated antibodies to IgG, IgM, IgA, C3, C1q, κ , and λ . In cases that lacked glomeruli in the frozen tissue, IF was performed on pronase-digested, paraffin-embedded tissue (pronase IF).⁸ Pronase IF for IgG, κ , and λ was also performed on FGN cases with apparent monotypic IgG staining on standard frozen tissue IF, as we have observed that some cases of FGN with light chain restriction on frozen tissue IF exhibit staining for both κ and λ on pronase IF.

Immunohistochemistry of DNAJB9

All instruments and reagents were purchased from Ventana Medical Systems, Inc. (Oro Valley, AZ) unless otherwise specified. DNAJB9 IHC was performed on 4- μ m-thick, formalin-fixed, paraffin-embedded tissue sections mounted on charged slides. Tissue slides were dried and melted in an oven at 68°C for 20 minutes. Slides were stained with an anti-DNAJB9 rabbit polyclonal antibody (catalog no. HPA040967; 1/75 titer; Sigma-Aldrich, St. Louis, MO) on a Ventana BenchMark XT system. The staining protocol included online deparaffinization, heat-induced epitope retrieval (HIER) with Ventana Cell Conditioning 1 solution (CC1) for 32 minutes, and incubation with the primary antibody for 32 minutes at 37°C. Antigen–antibody reactions were visualized using Ventana OptiView Universal DAB Detection and OptiView Amplification Kits. Counterstaining was performed online using Ventana Hematoxylin II for 8 minutes, followed by bluing reagent for 4 minutes. Two renal pathologists (S.H.N. and M.P.A.) independently evaluated the stained tissues for DNAJB9 positivity without knowledge of the diagnoses. The Mayo Clinic Institutional Review Board approved this study, which was conducted in accordance with the Declaration of Helsinki.

Immunoelectron Microscopy

Immuno-EM studies were done on 8 renal biopsy samples from patients followed up at University Hospital of Poitiers (different from the 214 Mayo clinic cases), including 3 cases of FGN, 3 cases of AL- λ amyloidosis, and 2 cases of immunotactoid glomerulopathy. Immuno-EM for DNAJB9 was performed using an anti-DNAJB9 rabbit polyclonal antibody (Sigma-Aldrich, St. Louis,

Table 1. Clinical and pathologic characteristics of 84 Mayo Clinic cases of fibrillary glomerulonephritis

Parameters	No. of patients (%)
Clinical features	
Female:male ratio	62/22 (74/26)
Mean age, yr (range)	59 (21–80)
Associated medical conditions	
Hypertension	52 (62%)
Diabetes mellitus	20 (24%)
Autoimmune disease ^a	12 (14%)
Malignancies ^b	8 (10%)
Hepatitis C infection	6 (7%)
Chronic obstructive pulmonary disease	6 (7%)
Kidney recipient	4 (5%)
Kidney donation	1 (1%)
Mean serum creatinine, mg/dl (range)	2.5 (0.4–12.8)
Renal insufficiency, serum creatinine > 1.2 mg/dl	58/82 (71%)
Mean 24-h urine protein, g/d (range)	5.1 (0–20)
Nephrotic range proteinuria, ≥ 3.0 g/d	52/80 (65%)
Full nephrotic syndrome ^c	21 (25%)
Microscopic hematuria	76 (90%)
Monoclonal protein on serum protein electrophoresis/immunofixation	3/71 (4%) ^d
Light microscopy	
Mean number of glomeruli sampled (range)	22 (2–101)
Globally sclerotic glomeruli, % (range)	29 (0–83)
Glomerular pattern of injury	
Mesangial proliferative	55 (65%)
Membranoproliferative	7 (8%)
Endocapillary proliferative	6 (7%)
Crescentic ^e	5 (6%)
Mesangial expansion without hypercellularity	11 (13%)
Crescents	23 (27%)
Tubular atrophy and interstitial fibrosis: none/mild/moderate/severe ^e	7/41/26/10 (8%/49%/31%/12%)
Concurrent glomerular disease	
Diabetic glomerulosclerosis	9 (11%)
Membranous nephropathy	2 (2%)
IgA nephropathy	2 (2%)
Transplant glomerulopathy	1 (1%)
Immunofluorescence	
Positive immune reactants in glomeruli, mean intensity if positive ^f	
IgG	84 (100%), 2.5+
IgM	52/83 (63%), 0.9+
IgA	17/83 (20%), 1.1+
C3	79/83 (95%), 2+
C1q	30/83 (36%), 1+
κ	80 (95%), 1.8+
λ	77/83 (93%), 2.1+
Polytypic IgG (i.e., +IgG, κ , and λ) ^g	75/83 (90%)
Monotypic IgG (i.e., +IgG and κ or IgG and λ) ^g	6/83 (7%)
γ Chain IgG only (i.e., +IgG with $-\kappa$ and $-\lambda$) ^h	2 (2%)
Extraglomerular staining for IgG	41 (49%)
Electron microscopy	
Location of fibrils	
Mesangial	84 (100%)
Glomerular capillary wall	79 (94%)

Table 1. (Continued)

Parameters	No. of patients (%)
Extraglomerular	16 (19%)
Mean diameters of fibrils (range of means)	16 (12–26)

^aSystemic lupus erythematosus (n = 3), rheumatoid arthritis (n = 2), idiopathic thrombocytopenic purpura (n = 2), sarcoidosis (n = 2), primary biliary cirrhosis (n = 1), primary sclerosing cholangitis (n = 1), and ankylosing spondylitis (n = 1).

^bLymphoma (n = 2), breast carcinoma (n = 2), thyroid carcinoma (n = 1), hepatocellular carcinoma (n = 1), prostate carcinoma (n = 1), and polycythemia vera (n = 1).

^cDefined by the presence of nephrotic range proteinuria, hypalbuminemia (serum albumin < 3.5 g/dl), and peripheral edema.

^dOne additional patient (who had positive glomerular staining for IgG and negative staining for κ and λ) had negative serum protein electrophoresis with immunofixation but had an IgG band on urine protein electrophoresis, low serum free κ -to- λ ratio, and 7% λ -restricted plasmacytosis on bone marrow biopsy.

^eDefined by the presence of crescents and/or necrosis affecting $\geq 50\%$ of nonsclerotic glomeruli.

^fScale: trace (0.5+), 1–3+.

^gNo glomeruli available for immunofluorescent staining for λ in 1 case.

^hBy both frozen tissue immunofluorescence and pronase immunofluorescence.

MO) and a gold-conjugated goat anti-rabbit IgG as a secondary antibody (Sigma-Aldrich Chimie, Saint Quentin Fallavier, France).⁹ Negative controls (i.e. by omitting the primary antibody) were run in parallel and demonstrated an absence of nonspecific staining with the gold-conjugated secondary antibody.

Positive controls were done using an anti- λ antibody (in AL amyloidosis and immunotactoid glomerulopathy cases) and an anti-IgG antibody (in FGN cases). Immuno-EM for IgG and λ light chain was performed using polyclonal anti- γ and anti- λ rabbit anti-human antibodies (Dakopatts), and a gold-conjugated goat anti-rabbit IgG as a secondary antibody (Sigma-Aldrich Chimie, Saint Quentin Fallavier, France).

RESULTS

To determine the normal cellular distribution of DNAJB9, IHC staining was performed on tissue microarrays of normal tissues (Table 2). Positive cells had a granular cytoplasmic staining pattern. Homogeneous (smudgy) extracellular deposits were not observed in any of the normal tissues. We then performed IHC staining for DNAJB9 on 214 kidney tissue samples, including 84 biopsy samples with FGN, 21 biopsy samples with renal amyloidosis, 98 biopsy samples with a large variety of NFGNGDs, and 11 samples (8 biopsy and 3 nephrectomy) from subjects without renal pathology. Table 3 shows detailed data on the diagnoses in these cases. DNAJB9 IHC staining was reported as positive if there was smudgy glomerular extracellular staining (i.e., mesangial with/without glomerular capillary wall staining, corresponding to the smudgy glomerular IgG staining observed by IF) and as negative if there was no smudgy glomerular extracellular staining. There was 100% concordance rate between the 2 renal pathologists

Table 2. Immunohistochemical expression of DNAJB9 in normal tissue

Organ system	Location of DNAJB9 positivity
Central nervous system	
Cerebral cortex	Neurons (variably fine to coarsely granular CS)
Digestive system	
Stomach, small and large intestine	Entero-endocrine cells (coarsely granular CS); Epithelial cells (finely granular CS)
Liver	Sinusoidal endothelial cells (variably fine to coarsely granular CS)
Pancreas	Acinar cells (variably fine to coarsely granular CS)
Respiratory system	
Lung	Epithelial cells (finely granular CS)
Endocrine system	
Pituitary (adenohypophysis)	Subset of adenohypophysal cells (variably finely to coarsely granular CS)
Thyroid	Epithelial cells (finely granular CS)
Parathyroid	Endothelial cells (finely granular CS)
Adrenal	Secretory cells of medulla (variably fine to coarsely granular CS)
Lymphoid system	
Spleen	Splenic cord (variably finely granular CS)
Tonsil	Small lymphocytes (variably finely granular CS)
Lymph node	Small lymphocytes of paracortex (variably finely granular CS)
Thymus	Small lymphocytes in the medulla (finely granular CS)
Female reproductive system	
Endometrium, Fallopian tube	Epithelial cells (finely granular CS)
Ovary	Endothelial cells (finely granular CS)
Placenta (term)	Syncytiotrophoblasts (variably finely granular CS)
Mammary glands	Alveolar and ductal epithelial cells and myoepithelial cells (finely granular CS)
Male reproductive system	
Testis	Primary spermatocytes and spermatids (finely granular CS)
Prostate	Fibromuscular stroma (finely granular CS)
Urinary System	
Kidney	Tubular epithelium and podocytes and mesangial cells and endothelial cells (variably finely granular CS), vascular smooth muscle cells
Ureter	Smooth muscle cells and urothelium (finely granular CS)
Skeletal muscle	(finely granular CS)

CS, cytoplasmic staining.

who reviewed the slides. We found strong smudgy DNAJB9 staining of the glomerular extracellular deposits in all cases of FGN (with 2 exceptions, discussed below), which was not present in any case of amyloidosis, NFGNGDs (with 1 exception, discussed below), or in healthy individuals (sensitivity of 97.6%, specificity of 99.2%). [Figure 1](#) shows examples of IHC results from FGN, normal, and amyloidosis kidney biopsy samples. [Figure 2](#) shows low-power representative images of DNAJB9 IHC results for some cases of NFGNGDs. [Supplementary Figure S1](#) shows high-power representative images of DNAJB9 IHC results for FGN, NFGNGDs, and amyloidosis.

Table 3. Diagnoses of 214 Mayo Clinic cases analyzed by immunohistochemistry

No. of cases	Renal FGN amyloidosis	Other glomerular disease (NFGNGDs)	Normal subjects
	84	21	98
	9 AL- λ	17 Smoking- and hypertension-related mesangial sclerosing glomerulopathy	11
	3 AL- κ	10 Diabetic glomerulosclerosis	
	2 AHL	9 Immunotactoid GN	
	1 AH	7 Proliferative lupus nephritis	
	2 ALect2	7 Membranous nephropathy	
	2 AA	6 Cryoglobulinemic GN	
	1 ALys	6 IgA nephropathy	
	1 AFib	5 Anti-GBM nephritis	
		4 Bacterial infection-associated GN	
		4 Monoclonal Ig deposition disease (2 γ heavy-chain deposition disease, 2 light-chain deposition disease)	
		4 Pauci-immune crescentic GN	
		4 Focal segmental glomerulosclerosis	
		3 C3 GN	
		3 Proliferative glomerulonephritis with monoclonal IgG deposits (PGNMID)	
		2 Minimal change disease	
		2 Transplant glomerulopathy	
		2 Thin basement membrane disease	
		1 Alport disease	
		1 Fibronectin glomerulopathy	
		1 Thrombotic microangiopathy	

FGN, fibrillary glomerulonephritis; GBM, glomerular basement membranes; GN, glomerulonephritis; NFGNGDs, non-FGN glomerular diseases.

The 2 DNAJB9-negative FGN cases were the only 2 cases in which the glomerular deposits stained only for IgG with negative staining for both κ and λ light chains on IF. DNAJB9 was positive in all 75 FGN cases (90%) with polytypic IgG (i.e., staining for IgG, κ , and λ) and in all 6 cases (7%) with monotypic IgG (i.e., staining for IgG and 1 light chain) ([Table 1](#)). Both patients with DNAJB9-negative FGN had clinical evidence of monoclonal gammopathy (detectable monoclonal protein in the serum and monoclonal plasmacytosis on bone marrow biopsy), whereas only 1 patient (17%) with monotypic FGN and 1 patient (1%) with polytypic FGN had clinical evidence of monoclonal gammopathy.

The single non-FGN case that was positive for DNAJB9 was a case of smoking and hypertension-related mesangial sclerosing glomerulopathy from a patient who also had hepatitis C virus (HCV) infection. In this case, there was very focal segmental smudgy DNAJB9 staining in 2 mesangial areas in a single glomerulus (out of 17 glomeruli sampled for LM), without glomerular IgG staining by IF or definitive evidence of FGN glomerular fibrillar deposits on EM. It is possible that this case represents a very early case of HCV-associated FGN in which the rare glomerular mesangial areas involved were not sampled for IF or EM. IHC staining for DNAJB9 was negative in 16 other cases of smoking and hypertension-related mesangial sclerosing glomerulopathy from non-HCV patients

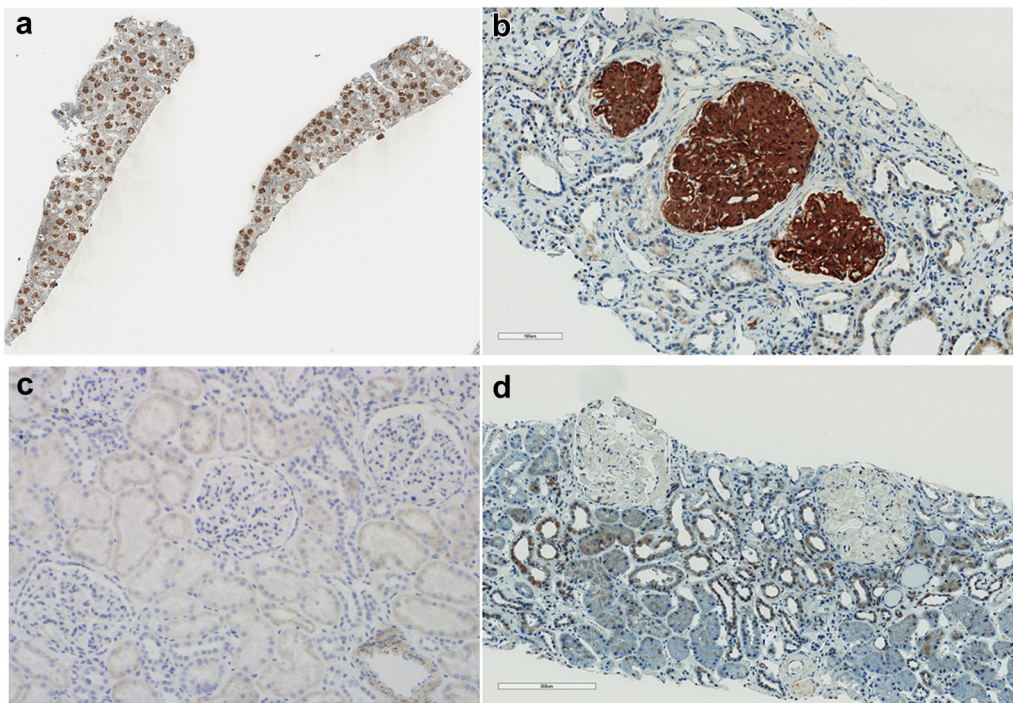


Figure 1. Immunohistochemistry (IHC) of DNAJB9 exclusively highlights fibrillary glomerulonephritis (FGN) glomeruli. (a,b) Immunohistochemistry shows strong glomerular staining for DNAJB9 in 2 different cases of FGN. (c) Normal and (d) κ light-chain amyloidosis do not show glomerular staining for DNAJB9. (a, Original magnification $\times 20$; b–d, original magnification $\times 200$.)

and in 2 cases of HCV-associated cryoglobulinemic glomerulonephritis.

In 71% of FGN cases (60/84), smudgy staining (similar in quality and intensity to the glomerular staining) was also observed in the extraglomerular compartments, including focal staining of tubular basement membranes (45%, 38/84 of cases), staining of the intima of very rare arterioles or arteries (42%, 35/84 of cases), and staining of the basement membranes of very rare peritubular capillaries (30%, 25/84 of cases) (Figure 3a, b). In 62% of these cases (37/60), focal smudgy to linear extraglomerular staining for IgG (weaker in intensity than the glomerular staining) was observed on IF (in a few tubular basement membranes, arterioles, and/or peritubular capillaries) (Figure 3d, e). Extraglomerular FGN fibrils were observed in 27% (16/60) of these cases on EM (involving a few tubular basement membranes in most cases, and involving rare arterioles, peritubular capillaries, or interstitium in a few cases) (Supplementary Figure S2). In 1 patient with FGN who underwent splenectomy for the treatment of idiopathic thrombocytopenic purpura, smudgy staining similar to the glomerular staining was observed extensively in splenic arterioles (Figure 3c), which also showed smudgy staining for IgG by pronase IF (Figure 3f), and randomly oriented fibrils by EM. No smudgy staining of tubular basement membranes, peritubular capillaries, or vessels for DNAJB9 was observed in any case of amyloidosis, NFGNGDs, or

healthy subjects (including in normal tissue microarrays).

Among the 214 Mayo Clinic cases analyzed by IHC, 7 FGN cases that were positive for DNAJB9 by IHC were also analyzed by LMD/MS-MS (which detected abundant DNAJB9 protein in glomeruli⁷), and 43 non-FGN cases (including 26 NFGNGDs, 12 amyloidosis, and 5 normal) were also analyzed by LMD/MS-MS (which did not detect DNAJB9 in glomeruli⁷). We also performed LMD/MS-MS on the 2 cases of FGN that were negative for DNAJB9 by IHC (which detected spectra for Ig γ heavy chain without spectra for DNAJB9 protein, data not previously reported).

Immuno-EM showed localization of DNAJB9 to FGN fibrils in all 3 cases of FGN (Figure 4, Supplementary Figure S3), whereas no significant staining was observed in the 3 cases of AL amyloidosis or the 2 cases of immunotactoid glomerulopathy (Table 4, Supplementary Figure S3). As expected, the fibrils of FGN showed IgG and λ labeling, and the fibrils in AL- λ amyloidosis showed λ labeling (Table 4, Supplementary Figure S3). IHC performed on the 8 cases that underwent immuno-EM showed strong smudgy glomerular staining for DNAJB9 in all 3 FGN cases, whereas glomeruli in AL amyloidosis and immunotactoid glomerulopathy were negative (Supplementary Figure S4A). Furthermore, LMD/MS-MS performed on these 8 cases detected abundant DNAJB9 protein in glomeruli in the 3 FGN cases (Supplementary Figure S4B) but not in AL amyloidosis or

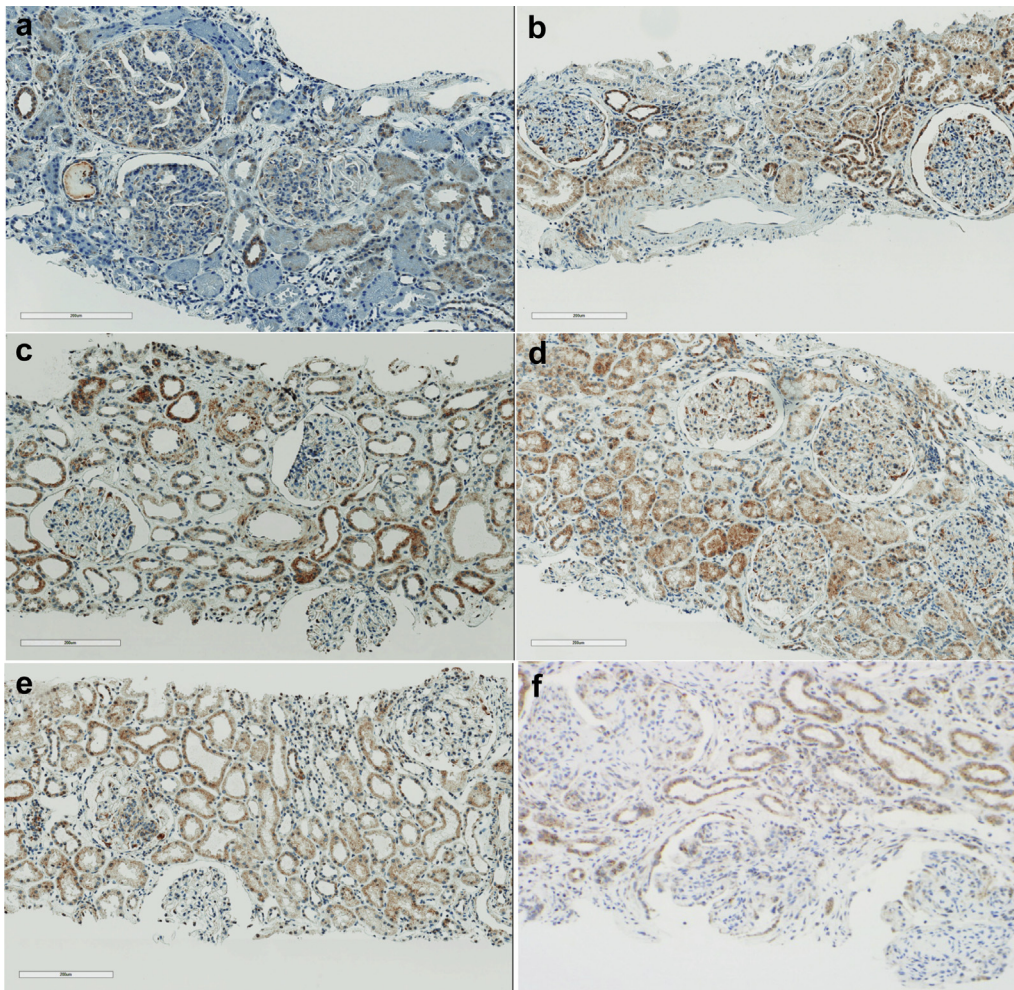


Figure 2. DNJB9 immunohistochemistry is negative in non-fibrillary glomerulonephritis renal biopsy samples. Staining for DNJB9 in bacterial infection-associated glomerulonephritis (GN) (a), diabetic glomerulosclerosis (b), membranous nephropathy (c), immunotactoid GN (d), lupus nephritis (e), and γ heavy-chain deposition disease (f). (Original magnification $\times 100$.)

immunotactoid glomerulopathy cases, supporting the findings observed by immuno-EM.

DISCUSSION

Currently, EM examination of glomeruli is required for diagnosing FGN. However, EM is not often available in pathology laboratories of developing countries because of its high cost. Even in developed countries (including some European countries), EM is not routinely performed in the evaluation of native kidney biopsy samples.¹⁰ Hence, FGN is likely an underdiagnosed disease. Our finding of abundant DNJB9 protein in glomeruli of 98% of FGN cases, but not in amyloidosis, non-FGN glomerular diseases, or normal glomeruli, indicates that testing for this biomarker is very valuable in the diagnosis of this rare disease. DNJB9 IHC is a quick and inexpensive tool that could be used by most clinical laboratories throughout the world. We found that even in early and subtle FGN cases that cannot be suspected by LM, DNJB9 IHC was positive

in some mesangial areas. DNJB9 IHC also helps to confirm the diagnosis of FGN in cases with a concurrent glomerular disease (which was present in 17% of our cases) (Table 1).

Importantly, we did not detect DNJB9 in cases of amyloidosis, diabetic nephropathy with fibrillosis, or fibronectin glomerulopathy, indicating that DNJB9 IHC can distinguish FGN from other kidney diseases that are characterized by glomerular fibrillar deposits. As glomerular fibrillar deposits are not specific for FGN, we propose changing the name of this disease to “DNJB9 fibrillary glomerulonephritis.” Of note, DNJB9 was not detected in 11 cases of immunotactoid glomerulopathy that were stained, supporting the current recommendation that FGN and immunotactoid glomerulopathy should not be lumped together as one disease because of different pathogenesis and notable differences in their clinical and pathologic characteristics.^{3,4,6,11}

DNJB protein family members are thought to act as co-chaperones to heat shock protein 70s (Hsp70s),

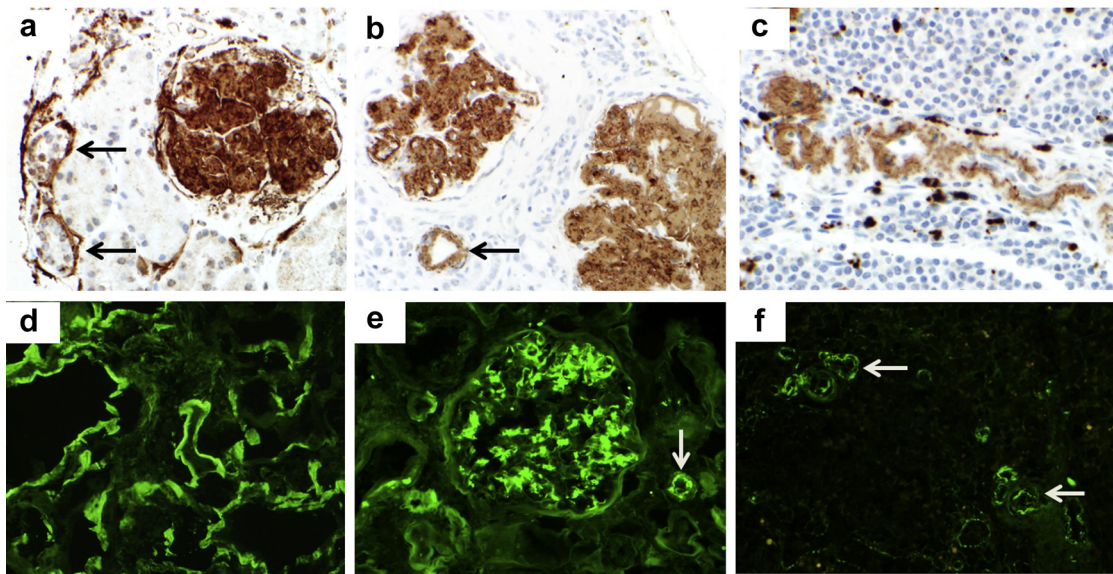


Figure 3. Extraglomerular deposits of DNAJB9 in fibrillary glomerulonephritis (FGN). (a) Focal smudgy staining of tubular basement membranes (arrows) similar to the glomerular staining. (b) Smudgy staining of an arteriole (arrow). (c) Smudgy staining of splenic arterioles. (d) Linear to smudgy staining of tubular basement membranes for IgG. (e) Smudgy staining on an arteriole (arrow) for IgG. (f) Splenic arterioles from the same specimen as in (c) show smudgy staining for IgG by pronase immunofluorescence (arrows). (a–e, Original magnification $\times 400$; f, original magnification $\times 200$.)

which are molecular chaperones important in proper folding, unfolding, translocation, or degradation of proteins. A total of 41 DNAJ/Hsp70s proteins have been identified in the human genome.¹² DNAJB9, also known as Mdg-1 or ERdj4, is a member of this family discovered in 2002¹³ and is localized to the endoplasmic reticulum (ER), where it interacts with BiP in the ER lumen and stimulates its ATPase activity. It is up-regulated in response to ER stress, suggesting that it might play a role in protein folding or ER-associated

protein degradation.^{13,14} DNAJB9 is expressed in all healthy tissues.¹³ We found variable (usually weak), finely granular cytoplasmic staining of tubular epithelial cells, glomerular cells, vascular smooth muscle cells, and rare interstitial inflammatory cells in many of our cases. This “background” granular staining should not be confused with the homogeneous smudgy and much more intense extracellular staining of glomerular deposits in FGN. Tubular casts and nerve bundles (when sampled) also showed nonspecific granular positivity for DNAJB9.

The pathogenesis of FGN is largely unknown. Because the glomerular deposits usually stain for IgG, κ , and λ but typically show IgG subtype restriction (usually IgG4), FGN is thought to represent an

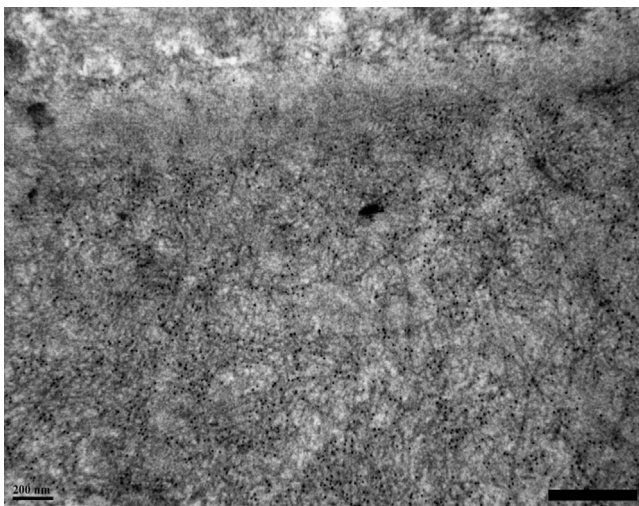


Figure 4. Ultrastructural immunohistochemical localization of DNAJB9 on fibrils of fibrillary glomerulonephritis (FGN). An immunoelectron microscopy micrograph from a patient with FGN (FGN 1 in Table 4) showing many gold particles labeling anti-DNAJB9 bound to FGN fibrils in the mesangium. (Original magnification $\times 60,000$.)

Table 4. Immunoelectron microscopy findings

Disease	Case No.	Staining intensity		
		DNAJB9	λ	γ
AL- λ amyloidosis	Case 1	Not significant	**	
	Case 2	Not significant	**	
	Case 3	Not significant	***	
FGN	Case 1	***		+
	Case 2	***		+
	Case 3	***		+
Immunotactoid GN	Case 1	Not significant	+	
	Case 1	Not significant	**	

FGN, fibrillary glomerulonephritis; GN, glomerulonephritis.

immune-complex type glomerulonephritis in which the IgG deposits are polymerized into fibrils (possibly due to their homogenous nature).⁴ Indeed, 2 immunoelectron microscopy studies have shown colocalization of IgG, κ , and λ to the individual FGN fibrils.^{15,16} However, without biochemical analysis of fibrils, these data do not unequivocally establish that the fibrils are composed of IgG, and it remains possible that IgG is secondarily bound to already formed fibrils comprised of a yet-to-be-determined precursor protein.¹¹ Considering the high abundance of DNAJB9 in FGN deposits and, as we showed in this study, its localization to individual FGN fibrils, DNAJB9 could potentially be the precursor fibril protein. It is possible that during ER stress, a misfolded DNAJB9 molecule is formed (possibly facilitated by protein post-translational modification) and deposited in glomeruli through entrapment and/or interaction with glomerular constituents, which then triggers an autoimmune response. Biochemical analysis of extracted fibrils from FGN patients, analysis of fibril structure, *in vitro* studies to investigate the kinetics of fibril formation, and determination of the source and triggers of DNAJB9 overexpression are needed to understand the etiology of FGN and the potential pathogenic role of DNAJB9 in this intriguing disease. Notably, we detected DNAJB9 not only in idiopathic FGN but also in FGN cases associated with HCV infection (n = 6), which could be due to DNAJB9 gene upregulation as part of the adaptation mechanisms to HCV-induced chronic ER stress,¹⁷ autoimmune disease (n = 12), malignancy (n = 8), and in FGN cases in the renal allograft (n = 4) (Table 1)

Interestingly, the 2 (2%) cases of FGN that were negative for DNAJB9 are unusual in that they stained for IgG only (without κ or λ light chains) on IF. Both cases were associated with clinical evidence of monoclonal gammopathy, whereas only 17% of the monotypic FGN patients and 1% of the polytypic FGN patients had clinical evidence of monoclonal gammopathy. It is possible that in these 2 cases of DNAJB9-negative “atypical” FGN, the fibrils are composed of a truncated Ig gamma heavy chain, similar to heavy chain amyloidosis and heavy chain deposition disease. Further studies are needed to confirm this theory.

DISCLOSURE

All the authors declared no competing interests.

SUPPLEMENTARY MATERIAL

Figure S1. High-power images of DNAJB9 immunohistochemistry (IHC) results. (A) Strong smudgy mesangial and

segmental glomerular basement membrane staining for DNAJB9 in a case of fibrillary glomerulonephritis (FGN) (original magnification $\times 600$). (B) Completely negative glomerular staining for DNAJB9 in a case of immunotactoid glomerulopathy (original magnification $\times 400$). (C) Nonspecific “background” (likely intracytoplasmic) granular staining for DNAJB9 in a case of IgA nephropathy (original magnification $\times 400$). This staining should be interpreted as negative for DNAJB9. (D) Nonspecific “background” granular staining for DNAJB9 in a case of fibrinogen α amyloidosis (original magnification $\times 400$). This staining should be interpreted as negative for DNAJB9. Amyloid deposits are largely negative.

Figure S2. Extraglomerular fibrillary glomerulonephritis (FGN) fibrils. The figure shows randomly-oriented straight fibrils within a thickened tubular basement membrane in a case of FGN. (Electron microscopy, original magnification $\times 15,000$; inset, original magnification $\times 50,000$).

Figure S3. Immuno-electron microscopy findings. (A) Gold particles labeling anti-DNAJB9 bound to fibrillary glomerulonephritis (FGN) fibrils (FGN #3 in Table 4, original magnification $\times 50,000$). (B) No significant staining of amyloid fibrils for DNAJB9 is observed (AL amyloidosis case #1 in Table 4, original magnification $\times 50,000$). (C) Anti-IgG antibody is localized to FGN fibrils (FGN #1 in Table 4, original magnification $\times 50,000$). (D) Anti- λ antibody is localized to amyloid fibrils (AL amyloidosis case #3 in Table 4, original magnification $\times 50,000$).

Figure S4. Immunohistochemical and proteomic findings in fibrillary glomerulonephritis (FGN) #2 patient in Table 4. (A) There is strong smudgy mesangial staining for DNAJB9 by immunohistochemistry (original magnification $\times 200$). (B) DNAJB9 expression in the same case. A single 10- μ m-thick section was obtained from the formalin-fixed, paraffin-embedded biopsy sample and mounted on a Director slide for laser microdissection of glomeruli. Two replicate dissections, each configured to collect glomeruli from a total area of 60,000 μ m², were performed. Proteins were extracted from the fragments of each dissection and digested using trypsin as previously described.¹⁸ Peptides were analyzed on a QExactive mass spectrometer using LC-MS/MS as previously described.¹⁹ Peptide tandem mass spectra (MS/MS) were processed using a previously described Bioinformatics pipeline²⁰ and proteins with at least two, unique, high confident (identification probability > 0.9) peptide identifications were considered to be present in the sample. The figure shows the number of MS/MS counts associated with each protein identification. DNAJB9 protein (FGN biomarker⁷) is highlighted with a blue star. We did not detect any amyloid tissue markers or type markers in this biopsy (data not shown).

Supplementary material is linked to the online version of the paper at www.kireports.org.

REFERENCES

1. Rosenmann E, Eliakim M. Nephrotic syndrome associated with amyloid-like glomerular deposits. *Nephron*. 1977;18:301–308.
2. Duffy JL, Khurana E, Susin M, et al. Fibrillary renal deposits and nephritis. *Am J Pathol*. 1983;113:279–290.
3. Bridoux F, Hugue V, Coldefy O, et al. Fibrillary glomerulonephritis and immunotactoid (microtubular) glomerulopathy are associated with distinct immunologic features. *Kidney Int*. 2002;62:1764–1775.
4. Fogo A, Qureshi N, Horn RG. Morphologic and clinical features of fibrillary glomerulonephritis versus immunotactoid glomerulopathy. *Am J Kidney Dis*. 1993;22:367–377.
5. Nasr SH, Valeri AM, Cornell LD, et al. Fibrillary glomerulonephritis: a report of 66 cases from a single institution. *Clin J Am Soc Nephrol*. 2011;6:775–784.
6. Rosenstock JL, Markowitz GS, Valeri AM, et al. Fibrillary and immunotactoid glomerulonephritis: distinct entities with different clinical and pathologic features. *Kidney Int*. 2003;63:1450–1461.
7. Dasari S, Alexander MP, Vrana JA, et al. DnaJ heat shock protein family member B9 is a biomarker for fibrillary GN. *J Am Soc Nephrol*. in press.
8. Nasr SH, Galgano SJ, Markowitz GS, et al. Immunofluorescence on pronase-digested paraffin sections: a valuable salvage technique for renal biopsies. *Kidney Int*. 2006;70:2148–2151.
9. Bridoux F, Sirac C, Hugue V, et al. Fanconi's syndrome induced by a monoclonal κ 3 light chain in Waldenstrom's macroglobulinemia. *Am J Kidney Dis*. 2005;45:749–757.
10. Pullman JM, Ferrario F, Nast CC. Actual practices in nephropathology: a survey and comparison with best practices. *Adv Anat Pathol*. 2007;14:132–140.
11. Alpers CE, Kowalewska J. Fibrillary glomerulonephritis and immunotactoid glomerulopathy. *J Am Soc Nephrol*. 2008;19:34–37.
12. Qiu XB, Shao YM, Miao S, Wang L. The diversity of the DnaJ/Hsp40 family, the crucial partners for Hsp70 chaperones. *Cell Mol Life Sci*. 2006;63:2560–2570.
13. Shen Y, Meunier L, Hendershot LM. Identification and characterization of a novel endoplasmic reticulum (ER) DnaJ homologue, which stimulates ATPase activity of BiP in vitro and is induced by ER stress. *J Biol Chem*. 2002;277:15947–15956.
14. Tsutsumi S, Namba T, Tanaka KI, et al. Celecoxib upregulates endoplasmic reticulum chaperones that inhibit celecoxib-induced apoptosis in human gastric cells. *Oncogene*. 2006;25:1018–1029.
15. Yang GC, Nieto R, Stachura I, Gallo GR. Ultrastructural immunohistochemical localization of polyclonal IgG, C3, and amyloid P component on the Congo red-negative amyloid-like fibrils of fibrillary glomerulopathy. *Am J Pathol*. 1992;141:409–419.
16. Casanova S, Donini U, Zucchelli P, et al. Immunohistochemical distinction between amyloidosis and fibrillar glomerulopathy. *Am J Clin Pathol*. 1992;97:787–795.
17. Merquiol E, Uzi D, Mueller T, et al. HCV causes chronic endoplasmic reticulum stress leading to adaptation and interference with the unfolded protein response. *PLoS One*. 2011;6:e24660.
18. Vrana JA, Gamez JD, Madden BJ, et al. Classification of amyloidosis by laser microdissection and mass spectrometry-based proteomic analysis in clinical biopsy specimens. *Blood*. 2009;114:4957–4959.
19. Nasr SH, Dasari S, Hasadsri L, et al. Novel type of renal amyloidosis derived from apolipoprotein-CII. *J Am Soc Nephrol*. 2017;28:439–445.
20. Theis JD, Dasari S, Vrana JA, et al. Shotgun-proteomics-based clinical testing for diagnosis and classification of amyloidosis. *J Mass Spectrom*. 2013;48:1067–1077.